Comparative Biochemistry and Physiology - Part D: Genomics and Proteomics 41 (2022) 100930

Contents lists available at ScienceDirect

Comparative Biochemistry and Physiology - Part D: Genomics and Proteomics

journal homepage: www.elsevier.com/locate/cbpd

Withering syndrome induced gene expression changes and a de-novo transcriptome for the Pinto abalone, *Haliotis kamtschatkana*

Alyssa R. Frederick [a,*], Joseph Heras [a,1], Carolyn S. Friedman [b], Donovan P. German [a]

[a] Department of Ecology and Evolutionary Biology, University of California, Irvine, 321 Steinhaus Hall, Irvine, CA 92697, USA
[b] School of Aquatic and Fishery Sciences, University of Washington, Box 355020, Seattle, WA 98195, USA

ARTICLE INFO

Edited by Chris Martyniuk

Keywords:
Disease
Digestive enzymes
Susceptibility
Gastropod

ABSTRACT

In the abalone and *Candidatus* Xenohaliotis californiensis (*Ca.* Xc) system, the *Ca.* Xc bacterium infects abalone digestive tissues and leads to extreme starvation and a characteristic "withering" of the gastropod foot. First identified in black abalone in California after an El Niño event, withering syndrome (WS) has caused large declines in wild black and captive white abalone on the northeastern Pacific coast, but disease resistance levels are species-, and possibly population-specific. This study compared gene expression patterns in the digestive gland of *Ca.* Xc-exposed and unexposed (control) Pinto abalone (*Haliotis kamtschatkana*), a particularly susceptible species. Lab-induced *Ca.* Xc infections were followed over 7 months and RNAseq was used to identify differential gene expression. Exposed Pinto abalone showed distinct changes in expression of 68 genes at 3 and 7 months post-infection relative to those in control animals. Upregulation of an orexin-like receptor (which is involved in feeding signaling) and a zinc peptidase-like region (many amino peptidases are zinc peptidases) in animals infected for 7 months indicates that animals with *Ca.* Xc infection may be starving and upregulating processes associated with feeding and digestion. Other groups of differentially expressed genes (DEGs) were upregulated or downregulated across control and exposed individuals over the 7-month experiment, including DEG groups that likely correspond to early disease state and to general stress response of being held in captivity. No patterns emerged in genes known to be involved in molluscan immune response, despite this being an expectation during a 7-month infection; digestion-related genes and unannotated DEGs were identified as targets for future research on potential immune response to WS in abalone.

1. Introduction

Beginning in 1985, populations of Black abalone (*Haliotis cracherodii*) began to decline along the California coastline, especially in the Channel Islands (Altstatt et al., 1996) due to the emergence of a new disease, withering syndrome (Haaker et al., 1992; Lafferty and Kuris, 1993; VanBlaricom et al., 1993; Tissot, 1995). It was later discovered that a Rickettsiales-like organism (RLO), a bacterial parasite, infects abalone digestive tissues and leads to starvation and a characteristic degradation of the gastropod foot (a disease called withering syndrome, or WS) (reviewed in Crosson et al., 2014). This RLO, first characterized in 2000 and since named *Candidatus* Xenohaliotis californiensis (*Ca.* Xc), is an intracellular bacterium from the family *Anaplasmataceae* with a unique 16S rRNA sequence of the bacterial taxon (Friedman et al., 2000; Cicala et al., 2017). The first histopathology analyses of the disease state in Black abalone showed that the bacterium formed inclusions throughout the digestive system, from the esophagus to the intestine. The most profound changes in the tissue occur in the digestive gland, where inclusions lead to metaplasia—the changing of secretory cells (that would otherwise secrete enzymes) to absorptive cells—and massive morphological changes of diverticula (Gardner et al., 1995). The resultant pedal atrophy was attributed to lack of nutrition due to morphological and functional changes in the digestive gland (Gardner et al., 1995), but digestive enzyme activity was not measured in the infected guts. A phage infected variant of the WS-RLO, referred to as RLOv, has distinct morphological differences in the size, shape and

Abbreviations: Ca. Xc, *Candidatus* Xenohaliotis californiensis; RLO, Rickettsiales-like organism; WS, withering syndrome; RLOv, phage infected variant of the WS-RLO; DEG, differentially expressed gene.

* Corresponding author at: Bodega Marine Laboratory, University of California, Davis, P.O. Box 247, 2099 Westshore Rd., Bodega Bay, CA, 94923, USA.
E-mail addresses: alyssarfrederick@gmail.com, abrac@ucdavis.edu (A.R. Frederick), carolynf@uw.edu (C.S. Friedman), dgerman@uci.edu (D.P. German).
[1] Present/Permanent Address: Department of Biology, California State University, San Bernardino, 5500 University Parkway, San Bernardino, CA 92407, USA

https://doi.org/10.1016/j.cbd.2021.100930
Received 10 August 2021; Received in revised form 29 September 2021; Accepted 1 November 2021
Available online 8 November 2021

staining characteristics (Friedman and Crosson, 2012), and results in lower mortality and host disease response than phage-free RLO infections in at least Black and Red abalone (Friedman et al., 2014a; Vater et al., 2018). In this study, we adopt the newer *Ca.* Xc nomenclature as a collective for both phage-infected and phage-free WS-RLOs in abalone guts linked to withering syndrome.

More holistic examinations of the physiological response of the abalone digestive system to *Ca.* Xc show that infected abalone experience reduction in growth, food intake, and metabolism (Gonzalez et al., 2012). Body mass decline, foot atrophy, higher mortality, and decreased glycogen stores in the foot muscle and digestive gland also appear as symptoms of the advanced stages of WS, and exposure to higher temperatures leads to significantly greater transmission of *Ca.* Xc to other abalone (Braid et al., 2005). In addition, elevated temperatures led to higher pathogenicity in Red abalone (*H. rufescens*) infected with *Ca.* Xc (Moore et al., 2000). Thus, the disease appears to be modulated in part by elevated temperatures, in response to which we see some abalone species showing marked increases in infection intensity and disease (Moore et al., 2000; Braid et al., 2005; Moore et al., 2011; Ben-Horin et al., 2013; Crosson and Friedman, 2018; Crosson et al., 2020). Interestingly, abalone in early stages of WS are able to repair early metaplastic damage if treated with oxytetracycline (in captivity), which stops bacterial growth and allows the host to remove *Ca.* Xc (Friedman et al., 2003, 2007).

Apart from the aforementioned morphological changes to the digestive system, the functional physiological changes (such as changes in gene expression similar to studies like McDowell et al., 2014) that occur during *Ca.* Xc infection, especially during sub-lethal stages of the disease, have not been extensively studied. For example, although it is known that the secretory tissue undergoes metaplasia, the degree to which this affects gene expression, and the related physiological processes encoded by those genes, in abalone digestive tissue is unknown. Here, we used transcriptomics to examine the gene expression patterns in unexposed and infected Pinto abalone (*H. kamtschatkana*) before and during *Ca.* Xc infection.

Pinto abalone are one of the species from the northeastern Pacific that are particularly susceptible (low resistance) to WS (Crosson and Friedman, 2018), making them an ideal test species for this study. Pinto abalone, as of April 2019, were listed as an Endangered species in the state of Washington (Carson and Ulrich, 2019) and WS was identified as a major threat to the species, making it even more critical that we understand how this disease impacts their physiology. In other species, such a Black abalone, WS has had severe impacts on populations. For example, WS is listed as a main contributing factor to the federal classification of Black abalone as “Endangered” as defined by the US Endangered Species Act of 1973 (ESA; Butler et al., 2009). All seven abalone species in California are culturally, economically, and ecologically important, making understanding the mechanisms that underlie WS essential to conserving these species and preserving this legacy.

All -omics tools, paired with other physiological measurements such as digestive function, disease load, and survival, contribute to a holistic understanding of the disease state and how it impairs physiological function (see Martin and Król, 2017). This combined approach can be especially useful when attempting to understand the complex interactions between host, pathogen, and environment (Gomez-Chiarri et al., 2015). For example, transcriptomic tools have been used to identify immune-related changes and function in response to pathogen challenges in bivalves, as well as the interaction of environmental impacts on disease resistance pathways (Gomez-Chiarri et al., 2015).

Transcriptome analysis during infection can also highlight organ-specific changes caused by disease. For instance, spring viremia of carp virus (SVCS) infections leads to differential gene expression changes in the brain and spleen of zebrafish, and these expression changes are associated with inflammation and metabolic pathways (Wang et al., 2017). These differentially expressed genes can have function or identity assigned to them, which would significantly improve understanding of the very fine ways in which pathogens alter host physiology, or pathways by which hosts respond to infectious agents. For example, an analysis of the transcriptomic response in grass carp intestines to *Aeromonas hydrophila* (a bacterial parasite) demonstrated that the intestinal tissue responded to infection with a large upregulation of immune-related pathways compared to other tissues (Song et al., 2017).

In this study, we used transcriptomics to determine the differentially expressed genes within the Pinto abalone digestive gland tissue, the target organ for disease-related changes during WS. Gene expression was compared during a 7-month WS challenge to improve our understanding of how WS progresses in this WS-susceptible abalone species. Our objective is to pinpoint physiological processes impacted during withering syndrome.

2. Methods

2.1. Infection experiment of Pinto abalone

RLO-free, captive-reared Pinto abalone ($n = 144$; mean shell length = 44.78 mm) were donated from the Puget Sound Restoration Fund. Red abalone ($n = 50$; mean shell length ~ 45 mm) were donated by The Abalone Farm, Inc. (Cayucos, CA). Prior to use in the study, feces from each red abalone group (infected and uninfected) for the head tanks were tested for RLO DNA presence using qPCR as described below (Friedman et al., 2014a). Abalone were held at the School of Aquatic and Fishery Sciences-University of Washington Pathogen Quarantine Facility. Abalone were acclimated over 2 weeks to the target experimental temperature of 18 °C and were maintained following the methods outlined in Friedman et al. (2014b). Briefly, abalone were divided into two re-circulating seawater systems (one control and one RLO-exposed) at the University of Washington, with 4 replicates per system and 18 animals per replicate (Fig. 1). Seawater was recirculated through a biological filtration (using 50 μm polystyrene media) followed by mechanical filtration (via a 25 μm pleated filter with activated carbon media) and UV-irradiation, and finally through a heat pump to maintain temperature (±0.5 °C) prior to re-entering each system through the head tank. Weekly water chemistry and abalone feedings were conducted using the methods of Friedman et al. (2014b). The control system head tank contained uninfected red abalone (control), while that in the RLO-

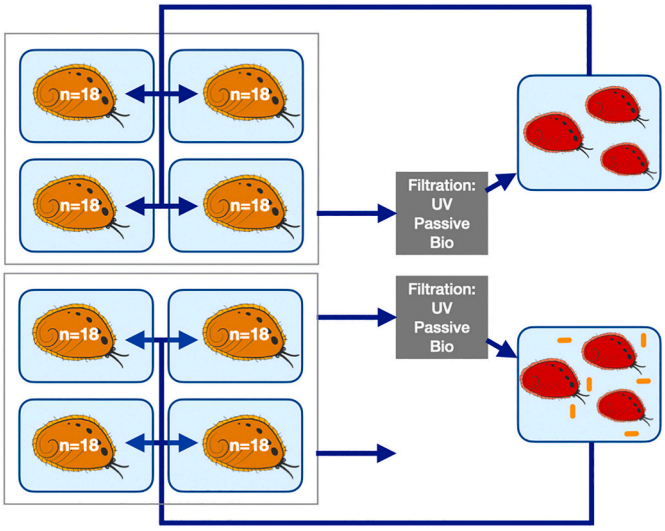

Fig. 1. Experimental design for Pinto abalone infection with WS
Pinto abalone were held in two separate tank systems with a head tank containing Red abalone. In the control treatment (top_, Red abalone were healthy, uninfected animals. In the experimental treatment (bottom), Red abalone were infected with *Ca.* Xc.

exposed head tank contained *Ca.* Xc-infected red abalone as a source of WS pathogen ($n = 18$ per head tank). Presence or absence of *Ca.* Xc (for experiment and control groups, respectively) was confirmed with qPCR, as described below. *Ca.* Xc was shed in the infected Red abalone feces (Crosson et al., 2014) and animals downstream were exposed to the bacterium. In a sampling scheme designed to emphasize early immune responses post-exposure to *Ca.* Xc, two animals from every replicate were sampled at $t = 0$ and post-exposure at 24 h, 3 days, 7 days, 6 weeks, 3 months, and 7 months. During each sampling, animals were euthanized by decapitation, dissected and post-esophageal (PE) and digestive gland (DG) tissue samples were taken and frozen in RNAlater and stored at −80 °C.

2.2. *Ca. Xc infection intensity of Pinto abalone (extraction and qPCR parameters)*

DNA was extracted by the Friedman lab from post-esophageal tissues bordering the digestive gland, as outlined in (Friedman et al., 2014a, 2014b). DNA was extracted from tissues using a QiaAmp DNA Stool Mini Kit (Qiagen Inc., Valencia, CA, USA) with modifications and parameters following (Friedman et al., 2014b). Extracted DNA was stored at −20 °C until qPCR analysis as described by (Friedman et al., 2014b) as follows: 25 μl reactions contained 12.5 μl 2x Immomix (Bioline USA Inc., Taunton, MA, USA), 320 nM of each primer, 200 nM of probe (Biosearch Technologies, Inc., Novato, CA, USA), 0.6 mg/μl BSA, 2 μl of DNA template, and sterile water to bring the final volume to 25 μl per reaction. Primers and probe for the WS-RLO were WSN1 F (AGT TTA CTG AAG GCA AGT AGC AGA), WSN1 R (TCT AAC TTG GAC TCA TTC AAA AGC) and WS-RLO_P (TGC TTG GAA ATC TAC TCA GAA GAC ATG A) (Friedman et al., 2014b). An initial denaturation incubation lasted 5 min at 95 °C, followed by 41 cycles of 95 °C for 15 s and 60 °C for 60 s. Samples were run in duplicates with a plasmid-based standard curve of known copy numbers for the *Ca.* Xc (WS-RLO) and *Ca.* Xc infected with a phage (RLOv) (Friedman et al., 2014a; Stanley et al. submitted). Histological examination of post-esophageal tissues stained with hematoxylin and eosin were collected, processed and examined according to Friedman et al. (2002).

2.3. *RNA extraction, cDNA preparation, and sequencing*

A 20–50 mg piece of tissue was excised from anterior portion of the of digestive gland (DG) adjacent to the right kidney. To identify differentially expressed genes between the control and infected individuals, RNA was extracted from the excised tissue from each individual for RNAseq (Garcia et al., 2012; Briscoe et al., 2013). Total RNA was extracted using TRIzol (Life Technologies, Grand Island, NY, USA) at University of California, Irvine (UCI) and purified with RNeasy spin columns (Qiagen Inc., Valencia, CA, USA). Some RNA samples were isolated at University of Washington (UW); RNA was isolated following the manufacturer's procotol for total RNA isolation from RNAzol RT and stored at −80 °C. Samples were checked for total RNA quality and concentration spectrophotometrically at the UCI Genomics High Throughput Facility. Criteria for choosing RNA samples for sequencing included a RIN score above 7 and RNA concentration above 50 ng/μl, with sufficient sample for Illumina prep and prioritizing pre-treatment, 3 month, and 7 month samples. Of the 53 samples with RNA extracted 17 samples met these criteria, so a TruSeq RNA sample prep kit (Illumina) was used to prepare individual cDNA libraries for 17 samples throughout the length of the experiment, according to the manufacturer's instructions. A cDNA concentration check before Illumina sequencing showed 3 of the 17 samples had low cDNA concentrations. Since we had funding for a full 20 samples, these 3 low-concentration samples were run in duplicate, after a second full cDNA prep per sample. However, these 3 low-concentration samples yielded poor quality sequences and were removed from further analysis, using the first preps for each sample. Therefore, the original 17 samples with high-quality, high-concentration RNA from the experiment were included in analysis. Seven samples were pre-exposure animals. Two samples were from animal exposed to *Ca.* Xc for 24 h. One sample was from an animal exposed to *Ca.* Xc for 3 months. Three samples were from control, unexposed animals after 7 months, and four samples were from animals exposed to *Ca.* Xc for 7 months. Re-purification was performed using Agencourt AMPure XP magnetic beads (Beckman Coulter Genomics). Quantification of the cDNA pool was performed with a Qubit 2.0 Flourometer, and cDNA was control-checked with an Agilent Bioanalyzer 2100. The cDNA was then normalized to 10 nM and run paired-end 100 bp runs on a HiSeq 4000 (Illumina, San Diego, CA) at the UCI Genomics High-Throughput Facility.

2.4. *Data analysis*

Raw data files were filtered and trimmed using Trimmomatic (0.35), which removed adapters, leading and trailing sequences below quality 3, reads with a 4-base sliding window where the quality fell below 15, and any reads less than 36 bases in length (Bolger et al., 2014). A de novo transcriptome was assembled using transcripts from 3 individuals, a control from the pre-exposure group, a control from the 7-month group, and an infected animal from the 7-month group. Transcript assembly was performed using Oases v0.2.08 (Schulz et al., 2012) in conjunction with Velvet v1.2.08 (Zerbino and Birney, 2008). All masked transcripts were annotated with the Trinotate annotation pipeline (v3.1.1; https://trinotate.github.io/; Bryant et al., 2017), which uses Swiss-Prot (Boeckmann et al., 2003), Pfam (Finn et al., 2014), eggnog v4.0 (Powell et al., 2014), Gene Ontology (Ashburner et al., 2000), SignalP v4.1 (Petersen et al., 2011), and Rnammer v1.2 (Lagesen et al., 2007). Gene ontologies were derived using NCBI BLAST and EMBL pfam databases. After assembly and annotation, Fragments Per Kilobase per Million (FPKM) were estimated for differential expression of the digestive gland genes in animals exposed to *Ca.* Xc and healthy, naïve (i.e. control; unexposed to *Ca.* Xc and uninfected) animals (using Trinity r2015–2.1.1). Unique genes differentially expressed between the two groups ($P < 0.001$) with at least a 4-fold difference were compared using a heat map generated in R v3.2.3 (https://www.r-project.org/) using Bioconductor v3.2 (Gentleman et al., 2004; Huber et al., 2015) and edgeR package (Robinson et al., 2010; McCarthy et al., 2012). Differential gene expression data was obtained for seven pre-exposure animals, two animals exposed to *Ca.* Xc for 24 h, one animal exposed to *Ca.* Xc for three months, four animals exposed to *Ca.* Xc for seven months, and three control animals in the experiment set-up after seven months. The clustering dendrogram groups transcripts by expression pattern. For example, transcripts that are upregulated in control animals but downregulated in experimental animals would be grouped together in the dendrogram. We labelled the main branches of the dendrogram (Fig. 3) with artificial group numbers to clarify discussion of these DEG groups.

2.5. *Gene prediction with Augustus*

DEGs in groups 1 (Low expression in pre-exposure & seven months) and 3a (High expression in 7-month infected animals) were mapped to the Red abalone (*H. rufescens*) genome from Masonbrink et al. (2019) using BLAST (blastn) v2.2.30 (Altschul et al., 1990) to further identify any unknown DEG functions in these groups. This allows for identification of conserved syntenic regions, and for locating loci (i.e. genes) that surround the unidentified DEGs, and thus, allows future analysis to reveal functional information and also whether these loci are conserved within *Haliotis* species. For DEGs with Red abalone genomic scaffold matches of greater than 90% identity, both the genomic Red abalone scaffold sequences and their corresponding Pinto abalone cDNA sequences were uploaded to Augustus v3.3.3, a gene prediction tool (Stanke et al., 2008) for prediction and annotation of coding genes in these genomic regions. Settings included reporting genes on both strands, with few alternative transcripts, and reference organism set to

Table 1
Infection metrics of *Ca.* Xc (both WS-RLO and RLOv types).

Metrics			Abalone Tissue Samples															
			Pre-Exposure							24 h Exposed		3 mo Exposed	7 mo Control			7 mo Exposed			
Assay	Tissue	Pathogen; Gene Expression	C-0-1	C-0-2	C-0-3	C-0-4	C-0-5	C-0-6	C-0-7	E-24h-1	E-24h-2	E-3mo-1	C-7mo-1	C-7mo-2	C-7mo-3	E-7mo-1	E-7mo-2	E-7mo-3	E-7mo-4
Histology	PE	RLO	0	0	0	0	0	0	0	0	0	1	0	0	0	0	2.5	0	2
		Phage	0	0	0	0	0	0	0	0	0	0	0	0	0	0	2	0	1
	DG	RLO	0	0	0	0	0	0	0	0	0	0	0	0	0	0	1.5	0	0
		Phage	0	0	0	0	0	0	0	0	0	1	0	0	0	1	1	0	0
*qPCR	DG	RLO	0	0	0	0	0	0	0	ND	ND	1.3E+01 (1.5E+0.0)	0	0	0	3.4E+02 (5.5E+0.0)	2.3E+04 (3.2E+03)	6.4E+0.0 (8E-01))	9.7E+01 (1.1E+01)
	DG	Phage	0	0	0	0	0	0	0	ND	ND	7.21E+0.0) (1.9E+0.0)	0	0	0	3.0E+06 (9.6E+04)	6.1E+06 (3.5E+05)	3.4E+03 (4.7E+02)	6.5E+02 (1.9E+01)
**RNA Expression	DG	Group 1	Down	Down	Down	Down	Down	Down	Down	Down	Up	Up	Up	Up	Up	Variable	Down	Down	Var-N/D
	DG	Group 2	Down	Variable	Down	Up	Up	Down	Up-Var	Up	Down	Up	Up-Var	Down	Up	Down	Down	Down	Down
	DG	Group 3a	Down	Down	Down	Down	Down	Down	Down	Neutral/ Down	Neutral/ Down	Up	Down	Down	Neutral/ Down	Up	Up	Up	Up
	DG	Group 3b	Down	Down	Down	Down	Down	Down	Down	Neutral/ Down	Neutral/ Down	Neutral/ Down	Up	Up	Neutral/ Down	Up	Up	Up	Up
	DG	Group 3c	Down	Down	Down	Down	Down	Down	Down	Up-Var	Up-Var	Up-Var	Variable	Up	Neutral/ Down	Up	Up	Neutral/ Up	Up
	DG	Group 4	Up	Variable	Down	Up	Down	Up	Up	Up	Up	Down	Down	Down	Down	Down	Down	Neutral	Down

Histology scores (Fig. 2) are shown for post-esophageal (PE) and digestive gland (DG), of both the RLO and RLOv ("Phage") type of *Ca.* Xc. *Copies/mg of tissue ± standard deviation for the RLO and Phage from qPCR reactions show the magnitude of infection in the animals. **Mean response trend of the differential gene expression analysis is included, with "Up" indicating relative upregulation of transcripts in that grouping, "Down" indicating downregulation, "Variable" indicating no pattern in expression, and Neutral/Up or Neutral/Down indicated a mixed response leaning towards either upregulation or downregulation (see Fig. 3). ND indicates no data collected.

Pisaster ochraceus. Any neighboring or overlapping coding sequences predicted by Augustus (Suppl. Fig. 1) were run through NCBI Nucleotide BLAST (blastx) database to infer functional relationships between the subject and query, and descriptions, total score, e-value, percent identity, and accession numbers of the top BLAST match (with a total score of at least 80) were recorded (Table 3). Only DEGs that mapped to the Red abalone genome, had Augustus matches that resulted in some annotation were included in the final Table 3. For comp81985, only 4 of the 52 matches were included, using the criteria of whether those Augustus suggestions overlapped with the cDNA sequence. This DEG was also annotated with Trinotate, and all annotation confirms the same gene identity for that DEG. For instances where there were many annotated matches, and the first match was a hypothetical or unannotated gene, the second match was recorded as long as the total score was also above 80.

3. Results

3.1. *Ca.* Xc infection intensity of Pinto abalone

Quantitative PCR (qPCR) data was analyzed using the number of copies of *Ca.* Xc DNA per reaction from duplicate replicates per sample and was used as a proxy for infection. Average copies/reaction and standard deviations are shown in Table 1. Both *Ca.* Xc (RLO) bacterial genes and RLOv copies/reaction were measured for select samples. Two of the control animals at 7 months that were used for the final transcriptome analysis showed no *Ca.* Xc (of WS-RLO or RLOv types) DNA amplification, confirming no contamination of control Pinto abalone with *Ca.* Xc. Data for all 4 infected animals at 7 months, and the one animal infected at 3 months, were included and amplification of *Ca.* Xc (both WS-RLO and RLOv types) suggested infection in all exposed animals at advanced timepoints (Table 1). These qPCR data confirm that only the exposed animals contained *Ca.* Xc DNA, while control animals remain uninfected throughout the experiment. Histological imaging visualized infections of primarily low to moderate intensity infections (scale of 1 on the histology scale of Friedman et al., 2002) in a pattern similar to the WS-RLO DNA amplified by qPCR (Table 1; Fig. 2). No abalone died or showed clinical signs of WS during the study.

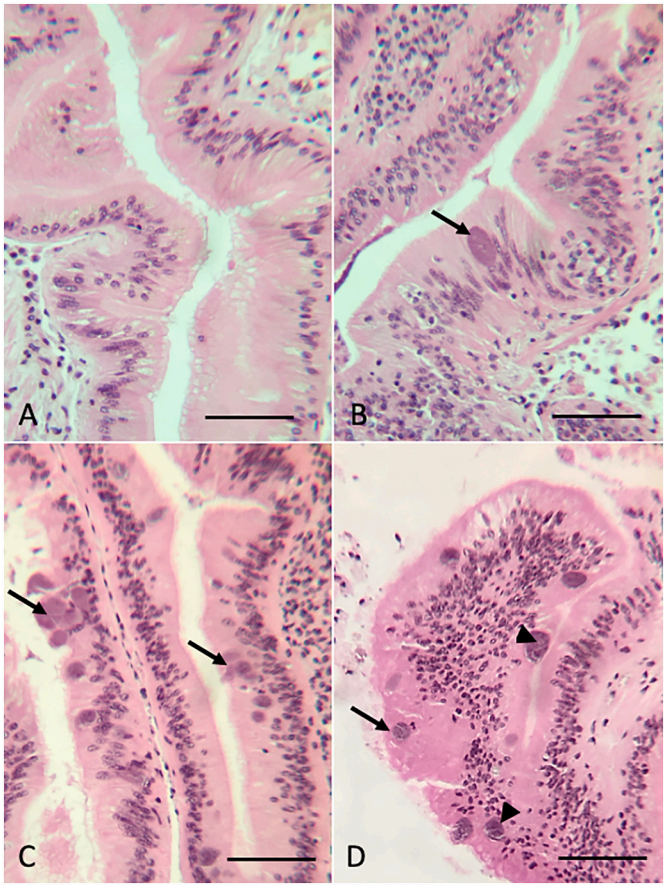

Fig. 2. Histological visualization of *Ca.* Xc infection intensity. Pinto abalone post-esophagus tissues stained with hematoxylin and eosin illustrating: A. Uninfected abalone; B. Abalone with a low intensity infection with *Ca.* Xc (arrow; histology scale = 1); C. Moderate infection with *Ca.* Xc (histology scale = 2); D. Light infection with *Ca.* Xc (scale = 1) and phage-infected *Ca.* Xc (arrowhead; scale = 1). Bars = 50 μm.

3.2. RNA extraction, cDNA preparation, and Pinto abalone transcriptome assembly

A final de novo transcriptome was assembled from 130,209 transcripts after trimming. Sixty eight genes were differentially expressed ($p = 0.001$) between pre-exposure, 24-h infected, 3-month infected, 7-month infected, and 7-month control individuals included in the analysis (see Fig. 3). Eighteen of the total 68 DEGs (26.5%) were identified with either annotation or gene ontologies, or both (see Table 2).

3.3. Patterns of gene expression in Pinto abalone infected with *Ca.* Xc

Sixty-eight genes (0.05% of the total number of transcripts sequenced) were differentially expressed with $p < 0.001$, and at least a 4-fold difference in expression. Heat map analysis was implemented to look for patterns in gene expression differences between treatment groups in $n = 17$ animals, across 7 months of infection.

DEG's were divided by lineage into 6 groups (Groups 1, 2, 3a, 3b, 3c, and 4) based on expression patterns (Fig. 3, Table 2), and given group descriptions to differentiate their observed expression patterns. Group 1 showed a pattern of DEGs that were downregulated in pre-exposure animals and exposed animals at seven months post-infection, relative to transcript expression of control animals at seven months, infected animals at 24 h post-infection, and three months post-infection. For ease of discussion, the pattern of expression in Group 1 was named “Low expression at pre-exposure and seven months.” Group 2's pattern, discussed as “Low expression at seven months,” featured downregulated DEGs in the 7-month infected animals relative to the majority of pre-exposure, 24-h infected, 3-month infected, and 7-month control animals, but variation with some individuals in each group showed relative downregulation of the transcripts in that cluster. Group 3 showed DEGs with three different patterns of regulation: one (Group 3a; High expression in 7-month infected animals) with strong upregulation of transcripts in the 7-month infected animals, and to a lesser degree, the 3-month infected individual. Another sub-cluster within Group 3 (Group 3b; High expression from seven months in the laboratory regardless of *Ca.* Xc infection) showed upregulation of transcripts in 7-month infected animals, and some upregulation in the majority of the 7-month control animals. Group 3c (High expression in infected animals) showed upregulation of 3 transcripts in infected animals at each timepoint. Group 4 (High expression in pre-exposure and early in the experiment) shows upregulation in a majority of the pre-exposure animals and in the 24-h infected animals, but downregulation in the rest of the individuals.

DEG's with bolded numbers to the right of the heatmap (Fig. 3) were identified with at least a gene ontology (GO) term or other functional annotation. Group 1 had one DEG for which the annotation suggested protein transport and signal transduction proteins. Group 2 had no annotated DEGs. Group 3a had one DEG involved in orexin reception and others involved in viral replication. Group 3b contained 6 annotated DEG's involved in various metabolic processes, including nitrogen and sulfur metabolism, cell structuring, and transport, among other functions (see Table 2 for a long list of gene ontology terms in these DEG's). Group 3c contained DEG's relating to peptidase activity and signal

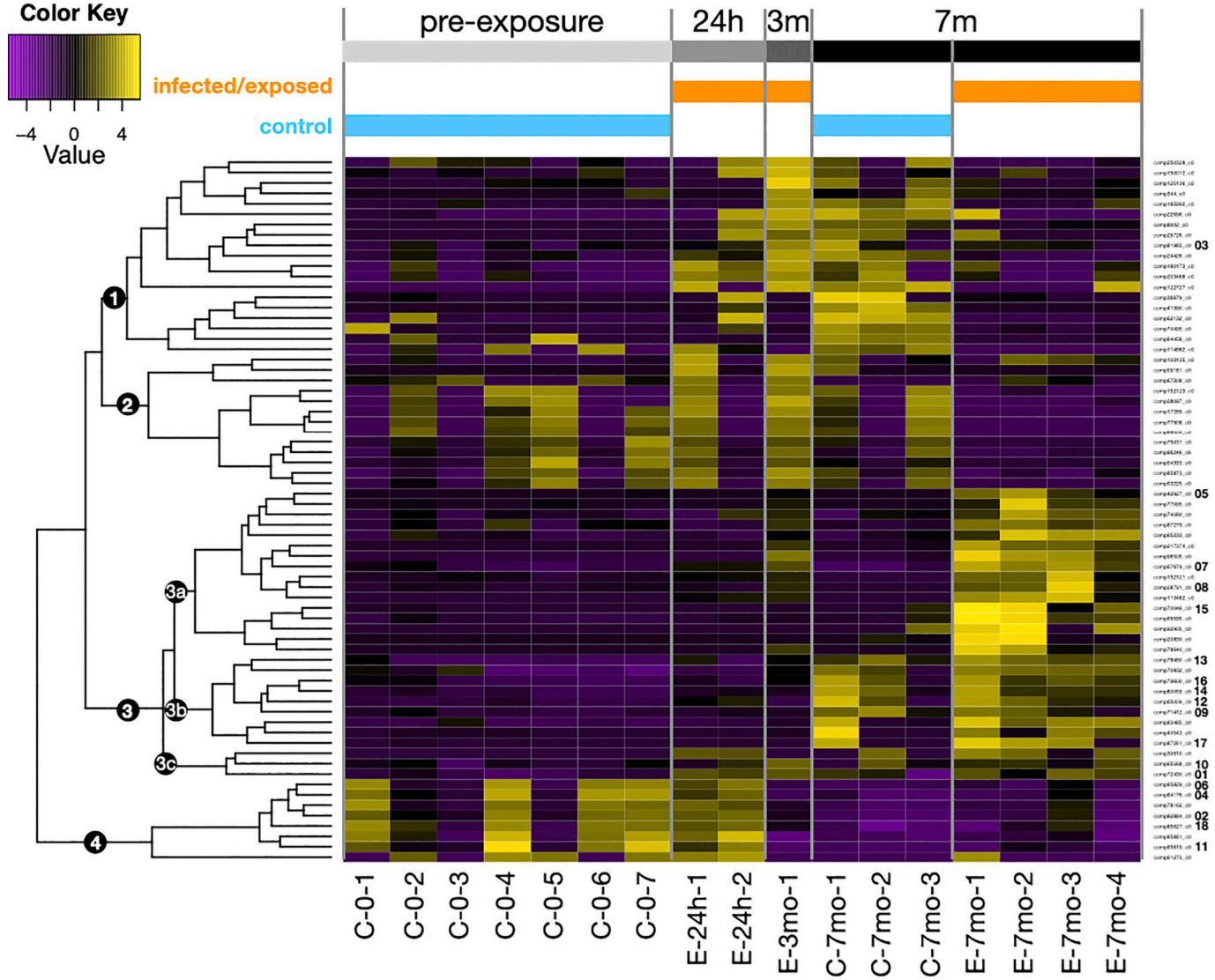

Fig. 3. Heatmap of differentially expressed transcripts in uninfected (control) Pinto abalone and abalone exposed to *Ca.* Xc over a 7-month experimental course. Four main clusters of differentially expressed genes (DEGs) were found among the $n = 17$ animals used in heatmap analysis, and annotated along the clustering dendrogram, which shows similarities in expression patterns between individuals. 18 DEGs were annotated and/or had GO terms attributed to them, and are labelled on the right by a gene ID # (See Table 2). Purple colors represent relative downregulation. Black represents neutral regulation relative to other animals. Yellow represents relative upregulation relative to other individuals. Animals are labelled as either C or E for control or infected/exposed (See Table 1), respectively. The middle portion of their IDs is the time they were sampled (e.g. 0 for $t = 0$ and 24 h for $t = 24$ h, etc.).

transduction. Group 4 had five annotated DEG's for which the functions were all related to membrane transport.

3.4. Gene prediction with Augustus

Of the 19 DEG's present in Group 1, 13 DEGs were successfully mapped to the Red abalone genome. Out of these 13 DEGs, Augustus was able to predict neighboring sequences, introns, or overlapping sequences for five fragments (Suppl. Fig. 1), all of which had matches in the NCBI Nucleotide blastx database (Table 3). These five DEGs included the one annotated DEG from the Trinotate search, an ADP-ribosylation factor. The Augustus matches confirm this gene identity. Of the remaining four sequences with Augustus findings, a neighboring gene included a cytochrome P450. An overlapping sequence was a 60S ribosomal protein (L13-like). One gene was identified as cation-dependent mannose-6-phosphate receptor-like, and the final Augustus match overlapped with genes in the transglutaminase family and SANT protein (Table 3).

Of the 16 DEG's present in Group 3a, six were successfully mapped to the Red abalone genome. Augustus predicted neighboring sequences, introns, or overlapping sequences for five of these six fragments (Table 3; Suppl. Fig. 1). Three of those five Augustus predictions had matches in NCBI Nucleotide blastx database. Of these three sequences with matches, one was also identified with the Trinotate methods above (comp42927), confirming the identity of an orexin receptor. One overlapping sequence matched mostly to hypothetical or uncharacterized proteins in a zinc peptidase-like region. The other overlapping sequence had one blastx match, a TCB2 transposase.

4. Discussion

Pinto abalone showed differential patterns of gene expression throughout the 7-month infection experiment. At both 3 and 7 months, all animals included in DEG analysis that were exposed to withering syndrome contained *Ca.* Xc DNA (Table 1), confirming that all Pinto abalone used in transcriptome analysis in the infected group indeed

Table 2
Gene annotation and biological process gene ontology terms for 18 differentially expressed genes.

Gene ID	Gene ID #	Heat Map Group	type of DE (C-0)	type of DE (C-7mo)	type of DE (E-7mo)	Annotation	GO: Biological Process
lcl|comp81985_c0	3	1	down	up	down	ADP-ribosylation factor 1-like2; GTP-binding protein	protein transport, small GTPase mediated signal transduction, vesicle-mediated transport
lcl|comp82884_c0	2	4	up/down	down	down	organic cation transporter 1; solute carrier family 22	carnitine transmembrane transport, determination of adult lifespan, organic cation transport
lcl|comp84176_c0	4	4	up/down	down	down	solute carrier family 22 member 15	ion transport, transmembrane transport
lcl|comp85829_c0	6	4	up/down	down	down	solute carrier family 22 member 6-A	transmembrane transport
lcl|comp85619_c0	11	4	up/down	down	down	monocarboxylate transporter 3	plasma membrane lactate transport, transmembrane transport
lcl|comp85627_c0	18	4	up/down	down	down	monocarboxylate transporter 6; major facilitator superfamily	plasma membrane lactate transport, transmembrane transport
lcl|comp42927_c0	5	3a	down	down	up	orexin receptor type 2	cellular response to hormone stimulus, circadian sleep/wake cycle process, feeding behavior, neuropeptide signaling pathway, phospholipase C-activating G-protein coupled receptor signaling pathway, regulation of circadian sleep/wake cycle, response to peptide, synaptic transmission, G-coupled receptor signaling pathway
lcl|comp67679_c0	7	3a	down	down	up	viral replicase polyprotein	DNA-templated transcription, viral genome replication
lcl|comp28791_c0	8	3a	down	down	up	viral structural polyprotein	–
lcl|comp70046_c0	15	3a	down	down	up	uncharacterized protein ORF91	–
lcl|comp71412_c0	9	3b	down	up	up	cysteine sulfinic acid decarboxylase	cellular nitrogen compound metabolic process, small molecular metabolic process, sulfur amino acid catabolic process, sulfur amino acid metabolic process, taurine biosynthetic process, carboxylic acid metabolism, cellular amino acid metabolic process
lcl|comp65009_c0	12	3b	down	up	up	A disintegrin and metalloproteinase with thrombospondin motifs; metallopeptidase with thrombospondin type 1 motif	cell migration, cell-matrix adhesion, cellular response to BMP stimulus, cellular response to interleukin-1, cellular response to tumor necrosis factor, negative regulation of cellular response to hepatocyte growth factor stimulus, negative regulation of cellular response to vascular endothelial growth factor stimulus, negative regulation of chondrocyte differentiation, negative regulation of hepatocyte growth factor receptor signaling pathway, proteoglycan catabolic process, proteolysis involved in cellular protein catabolic process, regulation of endothelial tube morphogenesis, regulation of inflammatory response, proteolysis
lcl|comp78480_c0	13	3b	down	up	up	collagen alpha-1(XIV) chain; cartilage matrix protein; growth plate cartilage chondrocute morphogenesis	chitin metabolic process
lcl|comp80059_c0	14	3b	down	up	up	A disintegrin and metalloproteinase with thrombospondin motifs gon-1	cell migration, ER to Golgi vesicle-mediated transport, gonad development, protein transport
lcl|comp79600_c0	16	3b	down	up	up	Neurotrypsin; protease	exocytosis, proteolysis
lcl|comp87261_c0	17	3b	down	up	up	viral structural polyprotein	DNA-templated transcription
lcl|comp72430_c0	1	3c	down	up/down	up	glutamyl endopeptidase; peptidase s1 and s6 chymotrypsin hap	–
lcl|comp65568_c0	10	3c	down	up/down	up	–	signal transduction

18 DEGs, labelled on the heat map in Fig. 3, had known gene annotations or gene ontology terms. The table summarizes the direction of differential expression for each DEG, the annotations from NCBI BlastX/BlastP and EMBL EggNOG, as well as gene ontology (GO) assignments from NCBI Blast and EMBL pfam. Where direction of differential expression is expressed as "up/down," individuals in each group were split roughly evenly between upregulation and downregulation of that particular gene.

Table 3
Augustus results for gene finding in DEGs from Groups 1 and 3a.

Red abalone genome mapping					BLAST (blastx) results					
DEG Group	DEG ID	Red Scaffold	% ID	Augustus finding	gene id (SF1)	Description	Total Score	*E*-value	Percent Identity	Accession Number
1	comp250328	83	95.56	2 neighboring sequences	g1.t1	cytochrome P450 26A1-like [*Crassostrea virginica*]	113	6.00E-26	40.41%	XP_022288365.1
					g2.t1	cytochrome P450 family 26 member 3 [*Branchiostoma lanceolatum*]	200	5.00E-57	45.93%	ANP24203.1
1	comp22696	37	97.06	3 neighboring sequences	g1.t1	–	–	–	–	–
					g2.t1	ribosomal protein rpl13 [*Eurythoe complanata*]	174	3.00E-53	74.55%	ABW23218.1
					g2.t2	ribosomal protein rpl13 [*Eurythoe complanata*]	174	6.00E-53	73.45%	ABW23218.1
1	comp81985	953	*99.26	52 overlapping sequences**	g16.t1	"ARF1_2" ADP ribosylation factor 1/2 [Mytilus coruscus]	259	6.00E-64	62.11%	CAC5393745.1
					g16.t2	"ARF1_2" ADP ribosylation factor 1/2 [Mytilus coruscus]	266	4.00E-67	65.79%	CAC5393745.1
					g21.t1	ADP-ribosylation factor [*Aplysia californica*]	179	3.00E-35	83.82%	XP_012935259.1
					g24.t1	ADP-ribosylation factor-like [*Pomacea canaliculata*]	209	3.00E-66	72.26%	XP_025076398.1
1	comp36679	202	*100	5 overlapping sequences and introns	g1.t1	cation-dependent mannose-6-phosphate receptor-like [*Lingula anatina*]	108	1.00E-24	41.61%	XP_023931076.1
					g1.t2	cation-dependent mannose-6-phosphate receptor-like [*Lingula anatina*]	108	1.00E-24	41.61%	XP_023931076.1
					g2.t1	–	–	–	–	–
					g3.t1	–	–	–	–	–
					g4.t1	uncharacterized protein LOC110466573 [Mizuhopecten yessoensis]	82.8	6.00E-16	41.59%	XP_021378830.1
1	comp41390	99	*98.8	8 overlapping sequences and introns	g1.t1	–	–	–	–	–
					g2.t1	SANT protein [*Atractosteus spatula*]	556	3.00E-26	38.11%	MBN3319760.1
					g2.t2	SANT protein [*Atractosteus spatula*]	544	9.00E-25	37.64%	MBN3319760.1
					g3.t1	"annulin-like" in transglutaminase family [Mizuhopecten yessoensis]	299	7.00E-92	54.41%	XP_021380405.1
					g4.t1	protein-glutamine gamma-glutamyltransferase K-like [*Patiria miniata*]	167	3.00E-42	35.00%	XP_038074044.1
					g4.t2	protein-glutamine gamma-glutamyltransferase K-like [*Patiria miniata*]	168	3.00E-42	35.00%	XP_038074044.2
					g5.t1	–	–	–	–	–
					g5.t2	–	–	–	–	–
3a	comp42927	693	*99.27	8 overlapping sequences and introns	g1.t1	gastrin/cholecystokinin type B receptor isoform X4 [*Aplysia californica*]	217	2.00E-61	33.81%	XP_005103731.1
					g2.t1	prisilkin-39-like isoform X3 [*Gouania willdenowi*]	524	6.00E-17	36.90%	XP_028309150.1
					g3.t1	orexin receptor type 2-like [*Pomacea canaliculata*]	131	2.00E-30	29.39%	XP_025092292.1
					g4.t1	–	–	–	–	–
					g5.t1	orexin receptor type 2-like [*Pomacea canaliculata*]	186	8.00E-30	29.34%	XP_025092292.1
					g5.t2	orexin receptor type 2-like [*Pomacea canaliculata*]	186	8.00E-30	29.34%	XP_025092292.1
					g6.t1	–	–	–	–	–
					g7.t1	orexin receptor type 2-like [*Crassostrea virginica*]	144	3.00E-35	31.81%	XP_022335491.1
3a	comp77095	1149	*100	14 overlapping sequences and introns	g1.t1	uncharacterized protein LOC112568058 [*Pomacea canaliculata*]	280	3.00E-88	97.00%	XP_025100866.1
					g1.t2	uncharacterized protein LOC112568058 [*Pomacea canaliculata*]	289	2.00E-89	44.96%	XP_025100866.1
					g1.t3	–	–	–	–	–
					g2.t1	–	–	–	–	–
					g2.t2	–	–	–	–	–
					g3.t1	sodium- and chloride-dependent glycine transporter 2-like [*Pecten maximus*]	82.4	3.00E-15	39.09%	XP_033738613.1
					g4.t1		300		48.41%	XP_025100866.1

(*continued on next page*)

Table 3 (*continued*)

Red abalone genome mapping					BLAST (blastx) results					
DEG Group	DEG ID	Red Scaffold	% ID	Augustus finding	gene id (SF1)	Description	Total Score	*E*-value	Percent Identity	Accession Number
						uncharacterized protein LOC112568058 [*Pomacea canaliculata*]		2.00E-94		
					g4.t2	uncharacterized protein LOC112568058 [*Pomacea canaliculata*]	289	4.00E-89	47.60%	XP_025100866.1
					g5.t1	unnamed protein product [Mytilus coruscus]	148	1.00E-26	57.75%	CAC5358245.1
					g6.t1	hypothetical protein DUI87_31074 [*Hirundo rustica rustica*]	175	2.00E-09	28.64%	RMB92524.1
					g7.t1	–	–	–	–	–
					g8.t1	hypothetical protein C0Q70_00134 [*Pomacea canaliculata*]	124	1.00E-30	40.27%	PVD37540.1
					g8.t2	uncharacterized protein LOC112568058 [*Pomacea canaliculata*]	145	4.00E-38	42.16%	XP_025100866.1
					g9.t1	Endo-1,4-beta-xylanase B [Mizuhopecten yessoensis]	8824	7.00E-31	53.73%	OWF43088.1
					g1.t1	–	–	–	–	–
					g2.t1	–	–	–	–	–
					g3.t1	–	–	–	–	–
					g4.t1	–	–	–	–	–
				6 overlapping sequences and introns	g5.t1	TCB2 transposase [*Polypterus senegalus*]	138	7.00E-37	49.62%	MBN3291941.1
3a	comp65233	188	*100		g6.t1	–	–	–	–	–

DEGs from Groups 1 and 3a were mapped to the Red Abalone genome, and corresponding Scaffold sequences are summarized. In sequences where more than one match was found within the same Red abalone scaffold, a single asterisk * indicates that the highest percent identity is shown in the table. Where the Pinto Abalone DEG did not map to the Red abalone genome, "-" is indicated for "Red Scaffold." Augustus gene tool v3.3.3 (Stanke et al., 2008) findings are summarized as either overlapping sequences with the Scaffold and/or cDNA DEG sequence, neighboring sequences, or introns (See Suppl. Fig. 1). In multiple DEGs, Augustus was unable to predict gene locations. Even where Augustus found results, the Augustus output did not always correspond to a match in the NCBI BLAST (blastx) database. Only DEGs which resulted in Augustus matches and a coding sequence match in the NCBI BLAST database were included in the table. Total score, e-value, percent identity, and accession number of matches are included. **comp81985 has 52 overlapping sequences. Only those with blastx matches are shown.

contained DNA of *Ca.* Xc (both the WS-RLO and RLOv forms). Histological examination confirmed *Ca.* Xc infections in abalone in which *Ca.* Xc DNA was amplified (Fig. 2). The infected animals, especially those at 7-months post-infection, also exhibited distinct patterns of gene expression compared to their 7-month control counterparts. During heatmap analysis, the DEGs were divided into 4 main groups, based on similarities in their expression patterns as demonstrated by dendrogram grouping (Table 2). Of the DEGs, 26.5% were annotated with function or gene ontology, which is comparable to a comparative transcriptome study of annelids where there was an annotation of 31.3–35.7% transcripts (Ribeiro et al., 2019).

4.1. DEGs: Group 1—low expression in pre-exposure & seven months

In Group 1 (Fig. 3, Table 2), relative downregulation of DEGs occurred in pre-exposure animals and infected 7-month animals. Upregulation of Group 1 DEGs occurred in 24-h exposed, 3-month exposed, and 7-month control animals. A possible explanation for the observed patterns of the downregulation of Group 1 genes in healthy animals, but upregulation of these genes throughout the experiment in both infected and uninfected animals, is that Group 1 genes may be upregulated in response to experimental/handling stress, or other conditions from living in captivity. However, the 7-month infected animals showed a unique downregulation in Group 1 DEGs, similar to the pre-exposure animals. If Group 1 genes, for example, were responsible for a normal stress response in the abalone, perhaps animals that are already fighting off a *Ca.* Xc infection and have been for 7 months, are not exhibiting appropriate stress responses that they would otherwise be able to exhibit without the additional burden of infection. Alternatively, some of the Group 1 genes may be downregulated similarly to the downregulation of ribonuclease inhibitors in herpesvirus-infected oysters (He et al., 2015; Guo and Ford, 2016). In this case, perhaps the Pinto abalone genes that normally inhibit immune or other disease-related responses are being downregulated in 7-month infected animals, perhaps as a consequence of WS, which may be a mechanism underlying high WS susceptibility in this species (Crosson and Friedman, 2018).

One of the DEGs in this first group (DEG #3 in Fig. 3 and Table 2) was identified as ADP-ribosylation factor 1-like 2, a GTP-binding protein, which, in humans, is involved in Golgi vesicle budding. Downregulation of ADP-ribosylation factor 1-like 2 in the 7-month infected animals (compared to 7-month control animals, Table 2) could result in less protein transport and changes to Golgi protein trafficking (Uniprot accession number **P84077**, Kahn et al., 1991). In mammal models, Golgi disassembly is a response to stress and can lead to cell death (Machamer, 2015), but this type of stress response process appears to be understudied or not examined in mollusks. Although only this one GTP-binding protein was able to annotated and assigned functional gene ontology (GO) information, downregulation may be a result of advanced WS disease state, suggesting that all of the Group 1 DEGs are an interesting target area for further exploration.

Augustus results suggest downregulation of a cytochrome *p*450 gene (Table 3), which are used in detoxification and have been identified in abalone as well as other marine invertebrates (Rewitz et al., 2006). In a study of rotifers, upregulation and downregulation of the different cytochrome p450s occurred in response to benzo[α]pyrene, a xenobiotic, exposure (Kim et al., 2017). The Augustus results, in conjunction with the gene expression data, also suggest a downregulation of genes near a 60S ribosomal protein gene (Table 3). Understanding which genes in the Pinto abalone DEGs were in close proximity to the identified 60S ribosomal gene could be important for understanding the physiological processes downregulated during advanced disease state. For example, another Augustus result suggests the downregulation of a gene in the transglutaminase family, which are a broad family of proteins with diverse functions, and may play a role disease development (Eckert

et al., 2014). Further exploration of these specific genes in abalone is needed to identify the processes possibly impacted by downregulation of transglutaminases in abalone. The sheer number of unnamed genes also leads us to call for more genomic resources in mollusks, especially in aquaculture contexts where selective breeding would be enhanced by this knowledge (Hollenbeck and Johnston, 2018).

4.2. DEGs: Group 2—low-expression at seven months

The Group 2 DEGs feature 13 genes that show greater variation in up- or down-regulation of DEGs within groups. However, the overall pattern is that these Group 2 DEGs are downregulated in the 7-month infected animals compared to all other groups. The DEGs in this group may be downregulated as a result of 7-month WS infections and may reflect gene expression changes at advanced stages of the disease. Group 2 is also an interesting target group for understanding genetic response to WS in Pinto abalone. In contrast to the observed differential expression of Group 1 genes which were downregulated in the 7-month infected group as well as the controls, those in Group 2 were mostly down-regulated only in the 7-month infected animals (but there were exceptions to this rule in pre-infected and control animals along the way; Fig. 3). Therefore, Group 2 genes may be involved in processes that are mostly inhibited or suppressed in long-term infected animals. Down-regulation of genes occurs in the immune response of other marine mollusks. For example, in oysters (*Crassostrea gigas*), some scavenger receptors and antioxidant genes are downregulated in response to Ostreid herpesvirus 1 (OsHV-1) infection (He et al., 2015; Guo and Ford, 2016). Unfortunately, none of the 13 DEGs in Group 2 could be annotated or assigned any functional GO terms, meaning they are not the same suites of genes observed to be downregulated in oyster (He et al., 2015; Guo and Ford, 2016). Thus, future work should focus on identifying what these genes are and in what metabolic pathways they are integrated, and again, require better molluskan genomic resources.

4.3. DEGs: Group 3—3a: high expression in 7-month infected animals; 3b: high expression from seven months in the laboratory regardless of Ca. Xc exposure; 3c: high expression in infected animals

The Group 3 DEGs are all downregulated in the pre-exposure animals. However, Subgroup 3a genes (High expression in 7-month infected animals; Fig. 3) are upregulated in the 7-month infected animals. These genes are an interesting area for further exploration for understanding Pinto abalone response to WS because they are uniquely upregulated only in long-term infected animals. These genes, therefore, may be activated in response to infection and demonstrate which genes are upregulated in response to long-term infection.

Of the four DEGs that have annotations in Subgroup 3a, two are of viral origin, one being a replicase polyprotein, which is associated with the biological process of viral replication, and the other a structural polyprotein. An NCBI BLAST query for both sequences in the NCBI nucleotide BLAST database and in the NCBI Virus database yielded no matches. Likewise, a PHASTER search yielded no phage genome matches (Zhou et al., 2011; Arndt et al., 2016). As the genome of the phage that infects *Ca.* Xc has been sequenced (Closek et al., 2016; Cruz-Flores et al., 2018), it is not likely that these viral sequences then are from the phage hyperparasite. Thus, they may be from a yet undescribed hyperparasite of the *Ca.* Xc or a viral parasite of the abalone that opportunistically impacts animals already stressed by withering syndrome (since it only appears upregulated in the 7-month infected animals). Alternatively, these genes could be of viral origin but now integrated into the abalone genome. In humans, the estimate is that 5–8% of our genetic content is of viral origin retrotransposed into the genome (Lander et al., 2001; Belshaw et al., 2004).

Of the other two DEGs with annotation in this subgroup, orexin receptor type 2 and uncharacterized protein ORF91 were upregulated only in the 7-month infected animals relative to the controls. The biological processes associated with orexin receptor type 2 include feeding behavior and cellular responses to hormones, among other processes (See Table 2 for full list). Orexin in mammalian systems regulate hunger and stimulate food consumption (Sakurai et al., 1998), so this upregulation of an orexin receptor in Pinto abalone is likely an attempt to stimulate feeding behavior. This suggests that physiological changes in the digestive gland associated with digestive dysfunction were apparent prior to abalone developing clinical disease. However, with impaired digestive function from WS, animals are unable to get nutrients from their food. Uncharacterized protein ORF91 is a protein found in chloroplasts, with currently uncharacterized biological function (Uniprot accession number **Q3BAI2**; Chang et al., 2006). It is likely that this protein being found here is the result of contamination from food in the digestive system of the sampled animals. The chloroplast protein may show patterns of upregulation on in the 7-month infected animals because the abalone digestive physiology may be altered from a 7-month infection. Deeper annotation of other genes, especially any related to digestive processes, would help clarify why this DEG demonstrates upregulation in *Ca.* Xc infected animals.

Augustus found two genes that overlapped the un-annotated DEGs in this group, as well (Table 3). One DEG overlap of the comp77095 sequence most often matched a hypothetical protein in a zinc peptidase-like region. While the specific protein is unclassified in detail, it is notable that many aminopeptidases, enzymes that cleave amino acids, are zinc peptidases (Taylor, 1993). As orexin is also upregulated, it is plausible that animals undergoing long-term infections may be attempting to stimulate feeding behavior *and* digestive processes that would allow them to gain more nutrients from their food. Targeting future studies to examine *Ca.* Xc impacts on abalone hormone signaling involved in hunger, as well as expression of digestive enzymes, would be especially informative in light of these results and the site of infection for CaXc lying in the digestive tract of abalone.

The DEGs in Subgroups 3b (Fig. 3) are upregulated in 7-month infected and control animals. These DEGs may be involved in the long-term response to life in captivity, such as a response to living in recirculating seawater or remaining on a consistent diet for months. Cysteine sulfinic acid decarboxylase is upregulated in all animals at 7 months and is associated with a variety of catabolic and metabolic processes, according to biological process gene ontology results (Table 2, #9). Captivity is known to have wide-reaching effects on metabolic processes in other animals (Palme et al., 2005). Mussels held in captivity experience metabolic changes similar to those experiencing starvation (Roznere et al., 2014), and similar stress responses may apply to abalone. The metallopeptidases upregulated in all 7-month animals (Table 2, #12 and #14) are associated with the inflammatory response and cell migration, and have been shown to be upregulated in other animals exposed to stress, such as a biocide exposure (Jia et al., 2011) but also in oysters in disease resistant lines exposed to diseases (McDowell et al., 2014). The protein associated with cartilage (Table 2, #13) has multiple possible identities, and all are related to growth and cell-cell organization of cartilage. The molluscan radula is composed largely of chitin on a cartilaginous base suggesting that up-regulation of DEG 13 may be related to chitin production induced by stress on the radula from scraping man made surfaces in captivity. A nonspecific neurotrypsin or protease is also upregulated in 7-month animals and is associated with exocytosis and proteolysis (Table 2, #16). A viral structural polyprotein, similar to those upregulated in Subgroup 3a was also found upregulated in both 7-month groups here (Table 2, #17). As this viral protein did not match any other BLAST results as well, the same discussion above may explain the presence of this gene here. Lastly, the peptidase (Table 2, #1) upregulated mostly in the 7-month infected and in some of the 7-month control animals may be a bacterial protein, but it is poorly characterized (Uniprot accession number **R4SR89**) and is therefore unremarkable here.

4.4. DEGs: Group 4—high expression in pre-exposure and early in the experiment

The Group 4 DEGs show mixed upregulation and downregulation in pre-exposure animals, but downregulation in both 7-month groups. These DEGs do not, therefore, elucidate any response to WS in Pinto abalone. According to the gene ontology for biological processes, all of the DEGs with annotations in this group are related to transmembrane transport. There are no strong patterns, however, between treatment groups for differential expression direction.

4.5. Conclusion & significance

This study explores patterns of differential gene expression involved in the long-term exposure to *Ca*. Xc in Pinto abalone. Different groups of transcripts show distinct regulation patterns, with some associated with life in captivity and others associated with long-term exposure to the disease WS. A few genes of particular interest function in hunger regulation and digestion. This work represents the first transcriptomic response to WS in Pinto abalone and highlights many areas for further exploration to understand this disease process. Deeper annotation and characterization of the Pinto abalone genome and transcriptome would help elucidate functional differences in infected and control animals. Future studies may consider comparing Pinto abalone response to closely related species with higher WS-resistance, such as Pink or Green abalone (Álvarez Tinajero et al., 2002; Moore et al., 2009). This study has identified at least 68 gene responses with differential expression between infected and control animals that warrant further study. In particular, examining the hunger and feeding behavior hormone signaling in conjunction with digestive enzyme and other digestive responses is important for understanding the molecular pathways impacted by *Ca*. Xc infection. Unlike disease responses in oyster, which has had many genes identified in the immune response (McDowell et al., 2014), there was no strong immune-related gene expression response found here. This warrants a call for an expansion of molecular research in abalone immune function. The intracellular location of the *Ca*. Xc bacteria may explain a lack of up-regulation in known immune genes as the bacteria may be effectively hidden from the host immune response (Thakur et al., 2019).

Because different species of abalone show differences in their susceptibility to withering syndrome (Crosson et al., 2014; Crosson and Friedman, 2018), transcriptomic analysis would be particularly useful if it could differentiate host species responses to bacterial challenges among different abalone taxa. Indeed, a case study on a bacterial pathogen of American oysters demonstrates how transcriptomics can be used to better understand resistance pathways in mollusks with severe diseases (McDowell et al., 2014). Like abalone responses to WS, oysters vary in their susceptibility to Roseovarius Oyster Disease (ROD). In short, inflammatory response and immune function genes were differentially upregulated in a resistant oyster line, supporting the hypothesis that resistance to this pathogen has a molecular underpinning (McDowell et al., 2014). Additionally, upregulated metabolic process genes in a susceptible oyster line support the hypothesis that a failed immune response against ROD places a large metabolic demand on the oysters, leading to their eventual death (McDowell et al., 2014). Studies like this one highlight the importance of understanding the molecular pathways that lead to disease states in marine organisms, and lead to a fervent call for better annotated molluscan genomes.

In study systems with varying susceptibility levels to a disease such as the *Haliotis* species in the northeastern Pacific with varying susceptibility to WS (Crosson and Friedman, 2018), understanding the differences in molecular responses to disease leads to an understanding of why and how closely related species are differentially susceptible or tolerant to diseases. However, to come to an understanding of differential resistance, the response to the disease itself in a susceptible species must be characterized before comparing with other, more resistant species. This study is the essential first step filling this knowledge gap of the gene expression response to *Ca*. Xc in abalone.

Supplementary data to this article can be found online at https://doi.org/10.1016/j.cbd.2021.100930.

Declaration of competing interest

The authors declare that they have no known competing financial interests or personal relationships that could have appeared to influence the work reported in this paper.

Data availability

Sequence data are available at NCBI BioProject Accession Number PRJNA778810 (https://www.ncbi.nlm.nih.gov/bioproject/PRJNA778810/).

Acknowledgements

The work presented here was conducted primarily on the occupied and unceded land of the Tongva and Acjachemen Nations. The authors acknowledge that they and their work have benefitted and continue to benefit from access to this land and the denial of these Nations from their traditional territories. We would like to thank Sean Bennett, Lisa Crosson and Sam White for running the Pinto abalone exposure study. We further thank Sam White for running all qPCR analyses and Michelle Herrera for her assistance in writing bioinformatics scripts. UCI undergraduate Avneet Kaur helped with RNA extraction and preparation.

Funding

This work was supported by a Sea and Sage Audubon Society Bloom-Hays Grant (ARF); University of California Irvine OCEANS Graduate Student Fellowship (ARF); University of California Irvine's Newkirk Center for Science and Society (ARF); the National Oceanic and Atmospheric Administration Grant No. NA14NMF4690293 to C. Friedman; the School of Aquatic & Fishery Sciences, University of Washington; the Western Society of Malacologists Research Grant (ARF); and the National Science Foundation Graduate Research Fellowship to ARF [Grant No. DGE-1321846].

References

Altschul, S.F., Gish, W., Miller, W., Myers, E.W., Lipman, D.J., 1990. Basic local alignment search tool. J. Mol. Biol. 215, 403–410.

Altstatt, J.M., Ambrose, R.F., Engle, J.M., Haaker, P.L., Lafferty, K.D., Raimondi, P.T., 1996. Recent declines of black abalone Haliotis cracherodii on the mainland coast of Central California. Mar. Ecol. Prog. Ser. 142, 185–192.

Álvarez Tinajero, M.D.C., Cáceres-Martínez, J., Gonzáles Avilés, J.G., 2002. Histopathological evaluation of the yellow abalone Haliotis corrugata and the blue abalone Haliotis fulgens from Baja California, México. J. Shellfish Res. 21, 825–830.

Arndt, D., Grant, J.R., Marcu, A., Sajed, T., Pon, A., Liang, Y., Wishart, D.S., 2016. PHASTER: a better, faster version of the PHAST phage search tool. Nucleic Acids Res. 44, W16–W21.

Ashburner, M., Ball, C.A., Blake, J.A., Botstein, D., Butler, H., Cherry, J.M., Davis, A.P., Dolinski, K., Dwight, S.S., Eppig, J.T., Harris, M.A., Hill, D.P., et al., 2000. Gene ontology: tool for the unification of biology. Nat. Genet. 25, 25–29.

Belshaw, R., Pereira, V., Katzourakis, A., Talbot, G., Paces, J., Burt, A., Tristem, M., 2004. Long-term reinfection of the human genome by endogenous retroviruses. P. Natl. Acad. Sc.i U. S. A. 101, 4894–4899.

Ben-Horin, T., Lenihan, H.S., Lafferty, K.D., 2013. Variable intertidal temperature explains why disease endangers black abalone. Ecology 94, 161–168.

Boeckmann, B., Bairoch, A., Apweiler, R., Blatter, M.C., Estreicher, A., Gasteiger, E., Martin, M.J., Michoud, K., O'Donovan, C., Phan, I., Pilbout, S., Schneider, M., 2003. The SWISS-PROT protein knowledgebase and its supplement TrEMBL in 2003. Nucleic Acids Res. 31, 365–370.

Bolger, A.M., Lohse, M., Usadel, B., 2014. Trimmomatic: a flexible trimmer for Illumina sequence data. Bioinformatics 30, 2114–2120.

Braid, B.A., Moore, J.D., Robbins, T.T., Hedrick, R.P., Tjeerdema, R.S., Friedman, C.S., 2005. Health and survival of red abalone, Haliotis rufescens, under varying temperature, food supply, and exposure to the agent of withering syndrome. J. Invertebr. Pathol. 89, 219–231.

Briscoe, A.D., Macias-Munoz, A., Kozak, K.M., Walters, J.R., Yuan, F.R., Jamie, G.A., Martin, S.H., Dasmahapatra, K.K., Ferguson, L.C., Mallet, J., Jacquin-Joly, E., Jiggins, C.D., 2013. Female behaviour drives expression and evolution of gustatory receptors in butterflies. PLoS Genet. 9.

Bryant, D.M., Johnson, K., DiTommaso, T., Tickle, T., Couger, M.B., Payzin-Dogru, D., Lee, T.J., Leigh, N.D., Kuo, T.-H., Davis, F.G., Bateman, J., Bryant, S., et al., 2017. A tissue-mapped axolotl De novo transcriptome enables identification of limb regeneration factors. Cell Rep. 18, 762–776.

Butler, J., DeVogelaere, A., Gustafson, C.M., Mobley, C., Neuman, M., Richards, D., Rumsey, S., Taylor, B., VanBlaricom, G., 2009. In: Commerce, D.O. (Ed.), Status Review for Black Abalone (Haliotis cracherodii Leach, 1814).

Carson, H.S., Ulrich, M., 2019. Status report for the pinto abalone in Washington, Olympia, WA.

Chang, C.C., Lin, H.C., Lin, I.P., Chow, T.Y., Chen, H.H., Chen, W.H., Cheng, C.H., Lin, C. Y., Liu, S.M., Chang, C.C., Chaw, S.M., 2006. The chloroplast genome of Phalaenopsis aphrodite (Orchidaceae): comparative analysis of evolutionary rate with that of grasses and its phylogenetic implications. Mol. Biol. Evol. 23, 279–291.

Cicala, F., Moore, J., Cáceres-Martínez, J., Del Río-Portilla, M., Hernández-Rodríguez, M., Vásquez-Yeomans, R., Rocha-Olivares, A., 2017. Multigenetic characterization of 'Candidatus xenohaliotis californiensis'. Int. J. Syst. Evol. Microbiol. 67 (1), 42–49.

Closek, C.J., Langevin, S., Burge, C.A., Crosson, L., White, S., Friedman, C.S., 2016. Genomic Characterization of a Novel Phage Found in Black Abalone (Haliotis cracherodii) Infected with Withering Syndrome pp ME44C-0875.

Crosson, L.M., Friedman, C.S., 2018. Withering syndrome susceptibility of northeastern Pacific abalones: a complex relationship with phylogeny and thermal experience. J. Invertebr. Pathol. 151, 91–101.

Crosson, L.M., Wight, N., VanBlaricom, G.R., Kiryu, I., Moore, J.D., Friedman, C.S., 2014. Abalone withering syndrome: distribution, impacts, current diagnostic methods and new findings. Dis. Aquat. Org. 108, 261–270.

Crosson, L.M., Lottsfeldt, N.S., Weavil-Abueg, M.E., Friedman, C.S., 2020. Abalone withering syndrome disease dynamics: infectious dose and temporal stability in seawater. J. Aquat. Anim. Health 32, 83–92.

Cruz-Flores, R., Caceres-Martinez, J., Del Rio-Portilla, M.A., Licea-Navarro, A.F., Gonzales-Sanchez, R., Guerrero, A., 2018. Complete genome sequence of a phage hyperparasite of Candidatus Xenohaliotis californiensis (Rickettsiales) - a pathogen of haliotis spp (Gasteropoda). Arch. Virol. 163, 1101–1104.

Eckert, R.L., Kaartinen, M.T., Nurminskaya, M., Belkin, A.M., Colak, G., Johnson, G.V.W., Mehta, K., 2014. Transglutaminase regulation of cell function. Physiol. Rev. 94, 383–417.

Finn, R.D., Bateman, A., Clements, J., Coggill, P., Eberhardt, R.Y., Eddy, S.R., Heger, A., Hetherington, K., Holm, L., Mistry, J., Sonnhammer, E.L., Tate, J., et al., 2014. Pfam: the protein families database. Nucleic Acids Res. 42, D222–D230.

Friedman, C.S., Crosson, L.M., 2012. Putative phage hyperparasite in the rickettsial pathogen of abalone, "Candidatus Xenohaliotis californiensis". Microb. Ecol. 64, 1064–1072.

Friedman, C.S., Andree, K.B., Beauchamp, K.A., Moore, J.D., Robbins, T.T., Shields, J.D., Hedrick, R.P., 2000. 'Candidatus Xenohaliotis californiensis', a newly described pathogen of abalone, Haliotis spp., along the west coast of North America. Int J Syst Evol Micr 50, 847–855.

Friedman, C.S., Biggs, W., Shields, J.D., Hedrick, R.P., 2002. Transmission of withering syndrome in black abalone, Haliotis cracherodii Leach. VIMS Articles 471. https://scholarworks.wm.edu/vimsarticles/471.

Friedman, C.S., Trevelyan, G., Robbins, T.T., Mulder, E.P., Fields, R., 2003. Development of an oral administration of oxytetracycline to control losses due to withering syndrome in cultured red abalone Haliotis rufescens. Aquaculture 224, 1–23.

Friedman, C.S., Scott, B.B., Strenge, R.E., Vadopalas, B., McCormick, T.B., 2007. Oxytetracycline as a tool to manage and prevent losses of the endandgered white abalone, *Haliotis sorenseni*, caused by withering syndrome. J. Shellfish Res. 26 (877-885), 879.

Friedman, C.S., Wight, N., Crosson, L.M., VanBlaricom, G.R., Lafferty, K.D., 2014a. Reduced disease in black abalone following mass mortality: phage therapy and natural selection. Front. Microbiol. 5.

Friedman, C.S., Wight, N., Crosson, L.M., White, S.J., Strenge, R.M., 2014b. Validation of a quantitative PCR assay for detection and quantification of 'Candidatus Xenohaliotis californiensis'. Dis. Aquat. Org. 108, 251–259.

Garcia, T.I., Shen, Y.J., Crawford, D., Oleksiak, M.F., Whitehead, A., Walter, R.B., 2012. RNA-seq reveals complex genetic response to Deepwater horizon oil release in Fundulus grandis. BMC Genomics 13.

Gardner, G.R., Harshbarger, J.C., Lake, J.L., Sawyer, T.K., Price, K.L., Stephenson, M.D., Haaker, P.L., Togstad, H.A., 1995. Association of prokaryotes with symptomatic appearance of withering syndrome in black abalone Haliotis cracherodii. J. Invertebr. Pathol. 66, 111–120.

Gentleman, R.C., Carey, V.J., Bates, D.M., Bolstad, B., Dettling, M., Dudoit, S., Ellis, B., Gautier, L., Ge, Y., Gentry, J., Hornik, K., Hothorn, T., et al., 2004. Bioconductor: open software development for computational biology and bioinformatics. Genome Biol. 5, R80.

Gomez-Chiarri, M., Guo, X.M., Tanguy, A., He, Y., Proestou, D., 2015. The use of -omic tools in the study of disease processes in marine bivalve mollusks. J. Invertebr. Pathol. 131, 137–154.

Gonzalez, R.C., Brokordt, K., Lohrmann, K.B., 2012. Physiological performance of juvenile Haliotis rufescens and Haliotis discus hannai abalone exposed to the withering syndrome agent. J. Invertebr. Pathol. 111, 20–26.

Guo, X.M., Ford, S.E., 2016. Infectious diseases of marine molluscs and host responses as revealed by genomic tools. Philos Trans. R Soc. B 371.

Haaker, P.L., Parker, D.O., Togstad, H., Richards, D.V., Davis, G.E., Friedman, C.S., 1992. Mass mortality and withering syndrome in black abalone, Haliotis cracherodii. In California. In: Shepherd, S.A., Tegner, M.J., Gusman del Proo, S.A. (Eds.), Abalone of the world: biology, fisheries and culture, Proceedings of the first international symposium on abalone. University Press, Cambridge, pp. 214–224.

He, Y., Jouaux, A., Ford, S.E., Lelong, C., Sourdaine, P., Mathieu, M., Guo, X., 2015. Transcriptome analysis reveals strong and complex antiviral response in a mollusc. Fish Shellfish Immunol. 46, 131–144.

Hollenbeck, C.M., Johnston, I.A., 2018. Genomic tools and selective breeding in molluscs. Front. Genet. 9.

Huber, W., Carey, V.J., Gentleman, R., Anders, S., Carlson, M., Carvalho, B.S., Bravo, H. C., Davis, S., Gatto, L., Girke, T., Gottardo, R., Hahne, F., et al., 2015. Orchestrating high-throughput genomic analysis with bioconductor. Nat. Methods 12, 115–121.

Jia, X., Zou, Z., Wang, G., Wang, S., Wang, Y., Zhang, Z., 2011. Gene expression profiling in respond to TBT exposure in small abalone Haliotis diversicolor. Fish Shellfish Immunol. 31, 557–563.

Kahn, R.A., Kern, F.G., Clark, J., Gelmann, E.P., Rulka, C., 1991. Human ADP-ribosylation factors. A functionally conserved family of GTP-binding proteins. J. Biol. Chem. 266, 2606–2614.

Kim, H.S., Han, J., Kim, H.J., Hagiwara, A., Lee, J.S., 2017. Identification of 28 cytochrome P450 genes from the transcriptome of the marine rotifer Brachionus plicatilis and analysis of their expression. Comp. Biochem. Physiol. Part D Genom. Proteom. 23, 1–7.

Lafferty, K.D., Kuris, A.M., 1993. Mass mortality of abalone Haliotis cracherodii on the California Channel Islands: tests of epidemiological hypotheses. Mar Ecol-Prog Ser 96, 239-239.

Lagesen, K., Hallin, P., Rødland, E.A., Staerfeldt, H.H., Rognes, T., Ussery, D.W., 2007. RNAmmer: consistent and rapid annotation of ribosomal RNA genes. Nucleic Acids Res. 35, 3100–3108.

Lander, E.S., Linton, L.M., Birren, B., Nusbaum, C., Zody, M.C., Baldwin, J., Devon, K., Dewar, K., Doyle, M., FitzHugh, W., Funke, R., Gage, D., et al., 2001. Initial sequencing and analysis of the human genome. Nature 409, 860–921.

Machamer, C.E., 2015. The Golgi complex in stress and death. Front Neurosci 9, 421-421.

Martin, S.A.M., Król, E., 2017. Nutrigenomics and immune function in fish: new insights from omics technologies. Dev. Comp. Immunol. 75, 86–98.

Masonbrink, R.E., Purcell, C.M., Boles, S.E., Whitehead, A., Hyde, J.R., Seetharam, A.S., Severin, A.J., 2019. An annotated genome for Haliotis rufescens (Red Abalone) and resequenced green, pink, pinto, black, and white abalone species. Genome Biol. Evol. 11, 431–438.

McCarthy, D.J., Chen, Y., Smyth, G.K., 2012. Differential expression analysis of multifactor RNA-seq experiments with respect to biological variation. Nucleic Acids Res. 40 (10), 4288–4297.

McDowell, I.C., Nikapitiya, C., Aguiar, D., Lane, C.E., Istrail, S., Gomez-Chiarri, M., 2014. Transcriptome of american oysters, Crassostrea virginica, in response to bacterial challenge: insights into potential mechanisms of disease resistance. Plos One 9, e105097.

Moore, J.D., Robbins, T.T., Friedman, C.S., 2000. Withering syndrome in farmed red abalone Haliotis rufescens: thermal induction and association with a gastrointestinal rickettsiales-like prokaryote. J. Aquat. Anim. Health 12, 26–34.

Moore, J.D., Juhasz, C.I., Robbins, T.T., Vilchis, L.I., 2009. Green abalone, Haliotis fulgens infected with the agent of withering syndrome do not express disease signs under a temperature regime permissive for red abalone, Haliotis rufescens. Mar. Biol. 156, 2325–2330.

Moore, J.D., Marshman, B.C., Chun, C.S.Y., 2011. Health and survival of red abalone Haliotis rufescens from San Miguel Island, California, USA, in a laboratory simulation of La Nina and El Nino conditions. J. Aquat. Anim. Health 23, 78–84.

Palme, R., Rettenbacher, S., Touma, C., El-Bahr, S.M., Möstl, E., 2005. Stress hormones in mammals and birds: comparative aspects regarding metabolism, excretion, and noninvasive measurement in fecal samples. Ann. N. Y. Acad. Sci. 1040, 162–171.

Petersen, T.N., Brunak, S., von Heijne, G., Nielsen, H., 2011. SignalP 4.0: discriminating signal peptides from transmembrane regions. Nat. Methods 8, 785–786.

Powell, S., Forslund, K., Szklarczyk, D., Trachana, K., Roth, A., Huerta-Cepas, J., Gabaldón, T., Rattei, T., Creevey, C., Kuhn, M., Jensen, L.J., von Mering, C., et al., 2014. eggNOG v4.0: nested orthology inference across 3686 organisms. Nucleic Acids Res. 42, D231–D239.

Rewitz, K.F., Styrishave, B., Lobner-Olsen, A., Andersen, O., 2006. Marine invertebrate cytochrome P450: emerging insights from vertebrate and insects analogies. Comp. Biochem. Physiol. C Toxicol. Pharmacol. 143, 363–381.

Ribeiro, R.P., Ponz-Segrelles, G., Bleidorn, C., Aguado, M.T., 2019. Comparative transcriptomics in syllidae (Annelida) indicates that posterior regeneration and regular growth are comparable, while anterior regeneration is a distinct process. BMC Genomics 20, 855.

Robinson, M.D., McCarthy, D.J., Smyth, G.K., 2010. edgeR: a bioconductor package for differential expression analysis of digital gene expression data. Bioinformatics 26 (1), 139–140.

Roznere, I., Watters, G.T., Wolfe, B.A., Daly, M., 2014. Nontargeted metabolomics reveals biochemical pathways altered in response to captivity and food limitation in the freshwater mussel Amblema plicata. Comp. Biochem. Physiol. - D: Genom. Proteom. 12, 53–60.

Sakurai, T., Amemiya, A., Ishii, M., Matsuzaki, I., Chemelli, R.M., Tanaka, H., Williams, S.C., Richardson, J.A., Kozlowski, G.P., Wilson, S., Arch, J.R.S., Buckingham, R.E., et al., 1998. Orexins and orexin receptors: a family of hypothalamic neuropeptides and G protein-coupled receptors that regulate feeding behavior. Cell 92, 573–585.

Schulz, M.H., Zerbino, D.R., Vingron, M., Birney, E., 2012. Oases: robust de novo RNA-seq assembly across the dynamic range of expression levels. Bioinformatics 28, 1086–1092.

Song, X., Hu, X., Sun, B., Bo, Y., Wu, K., Xiao, L., Gong, C., 2017. A transcriptome analysis focusing on inflammation-related genes of grass carp intestines following infection with Aeromonas hydrophila. Sci. Rep.U.K. 7, 40777.

Stanke, M., Diekhans, M., Baertsch, R., Haussler, D., 2008. Using native and syntenically mapped cDNA alignments to improve de novo gene finding. Bioinformatics 24, 637–644.

Stanley A. Langevin, Collin J. Closek, Colleen A. Burge, Roberto Cruz Flores, Samuel J. White, Lisa M. Crosson, Bryanda J. Wippel, Owen D. Solberg, and Carolyn S. Friedman. Unique microbial symbiosis between Xenohaliotis phage *attenuatum* and its host *Candidatus* Xenohaliotis californiensis. Mol. Ecol. (submitted).

Taylor, A., 1993. Aminopeptidases: structure and function. FASEB J. 7, 290–298.

Thakur, A., Mikkelsen, H., Jungersen, G., 2019. Intracellular pathogens: host immunity and microbial persistence strategies. J. Immunol. Res. 2019, 1356540.

Tissot, B.N., 1995. Recruitment, growth, and survivorship of black abalone on Santa Cruz Island following mass mortality. Bull. South. Calif. Acad. Sci. 94 (3), 179–189.

VanBlaricom, G.R., Ruediger, J.L., Friedman, C.S., Woodard, D.D., Hedrick, R.P., 1993. Discovery of withering syndrome among black abalone Haliotis cracherodii leach, 1814, populations at San Nicolas Island, California. J. Shellfish Res. 12, 185–188.

Vater, A., Byrne, B.A., Marshman, B.C., Ashlock, L.W., Moore, J.D., 2018. Differing responses of red abalone (Haliotis rufescens) and white abalone (H. sorenseni) to infection with phage-associated candidatus xenohaliotis californiensis. PeerJ 6, e5104.

Wang, Y., Zhang, H., Lu, Y., Wang, F., Liu, L., Liu, J., Liu, X., 2017. Comparative transcriptome analysis of zebrafish (Danio rerio) brain and spleen infected with spring viremia of carp virus (SVCV). Fish Shellfish Immunol. 69, 35–45.

Zerbino, D.R., Birney, E., 2008. Velvet: algorithms for de novo short read assembly using de Bruijn graphs. Genome Res. 18, 821–829.

Zhou, Y., Liang, Y., Lynch, K.H., Dennis, J.J., Wishart, D.S., 2011. PHAST: a fast phage search tool. Nucleic Acids Res. 39, W347–W352.